Efficiency of a two-stage heat engine at optimal power

I. Iyyappan and Ramandeep S. Johal

Department of Physical Sciences, Indian Institute of Science Education and Research Mohali
Sector 81, S. A. S. Nagar, Manauli PO 140306, Punjab, India

Abstract – We propose a two-stage heat cycle for an optimized linear irreversible heat engine. In the first stage, the heat engine works between the hot reservoir and a finite-sized sink. In the second stage, it works between the finite-sized heat source and cold reservoir. Under the tight-coupling condition, the engine shows the low-dissipation behavior in each stage, *i.e.*, the entropy generated depends inversely on the duration of the process. The phenomenological dissipation constants are determined within the theory itself in terms of the heat transfer coefficients and the heat capacity of the auxiliary system. We study the efficiency at maximum power and highlight a class of efficiencies in the symmetric case that show universality up to second order in Carnot efficiency, while the Curzon-Ahlborn efficiency is obtained as the lower bound for this class.

Introduction. – The central result in thermodynamics is that a reversible heat cycle between a hot and a cold reservoir achieves the Carnot efficiency [1]

$$\eta_{\mathrm{C}} = 1 - \frac{T_c}{T_h}, \tag{1}$$

where the temperatures of the reservoirs satisfy $T_c < T_h$. This result is outstanding for its independence from the nature of the working medium and the exact type of reversible cycle. Real-world machines mostly operate in irreversible regimes with efficiencies that are system and/or mechanism dependent [2–14]. Thus, it is remarkable to find universal features for efficiency in different models of irreversible machines [15–34].

Various models have been proposed in the literature, such as the endoreversible [2], stochastic [16,33] and the low-dissipation (LD) [19] ones, which work with a finite cycle time. Steady-state thermal machines have been studied using a linear irreversible framework [15] and beyond [21]. Although the formula rediscovered by Curzon and Ahlborn [2,25], $\eta_{\mathrm{CA}} = 1 - \sqrt{1 - \eta_{\mathrm{C}}}$, was initially suspected to be a generic result for efficiency at maximum power (EMP), it actually applies to small temperature gradients (small values of η_{C}), whereby $\eta_{\mathrm{CA}} \approx \eta_{\mathrm{C}}/2 + \eta_{\mathrm{C}}^2/8 + O[\eta_{\mathrm{C}}^3]$. The universal nature of the first- and the second-order terms has been subsequently elaborated in various models [16–18]. Apart from finite-rate mechanisms, models with finite-sized reservoir(s) have also been studied [35–40].

In this letter, we propose a two-stage linear irreversible heat engine which runs in a cycle. In the first stage, the heat engine works between the hot reservoir and a finite-sized sink (see fig. 1). In the second stage, it works between the finite-sized heat source and the cold reservoir. Our first main result shows that a linear irreversible engine with a finite-sized sink or source, and optimized for its performance in a given time, shows the LD behavior such that the total entropy generated in the process is inversely proportional to the duration of the process [19]. More precisely, the LD behaviour is obtained as a reasonable approximation to our model in the strong-coupling limit. The second main result is that, under a condition of symmetry, we obtain a class of efficiencies showing universality up to the second order in the Carnot value. Interestingly, CA-efficiency emerges as the lower bound of this class (see eq. (30)).

Let us first consider the work extraction by *reversible* means. We denote the energy and entropy of the system by (U_h, S_h) and (U_c, S_c), at temperature T_h and T_c, respectively. Also, we denote the heat capacity at constant volume of the finite-sized heat sink/source as $C_V(T)$ and it is a function of temperature T. For simplicity, we take the volume of the finite-sized heat source or sink to be constant during the cycle. In the first stage, the finite-sized heat sink is initially at temperature T_c, and it is coupled with the hot reservoir through a heat engine. The engine extracts work reversibly via infinitesimal heat cycles. The heat ejected towards the finite-sized sink successively
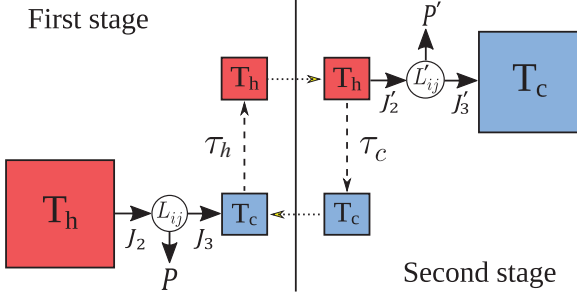
Fig. 1: The schematic diagram of a two-stage heat engine. In the first stage, the hot reservoir (T_h) is coupled with a finite-sized sink (blue box initially at temperature T_c) via a linear irreversible heat engine. After time τ_h, the temperature of the sink reaches T_h. In the second stage, the finite-sized heat source (red box initially at temperature T_h) is coupled with the cold reservoir (T_c) via a linear irreversible heat engine. After time τ_c, the finite-sized heat source comes back to its initial state of the first stage, thus completing a cycle.

increases its temperature until it attains thermal equilibrium with the hot reservoir. The maximum extracted work, also called exergy [41], in the first stage, is then $W_1 = T_h \Delta S - \Delta U$. Here, $\Delta X = X_h - X_c$. In the second stage, the system is detached from the previous set-up and coupled to the cold reservoir via a reversible heat engine. Again, work can be obtained till thermal equilibrium is achieved with the cold reservoir, completing one cycle for the auxiliary system. So, the energy in the second stage is $W_2 = \Delta U - T_c \Delta S$. The total work extracted in one cycle is $W_0 \equiv W_1 + W_2 = \Delta T \Delta S$. The input heat extracted from the hot reservoir is $Q_h = T_h \Delta S$. So, the efficiency $\eta = W_0/Q_h$, as expected, is equal to the Carnot value. Note that, since the auxiliary system interpolates between two given initial and final equilibrium states, ΔU and ΔS are given parameters of the cycle.

Linear irreversible heat engine. – Such an engine is in simultaneous contact with both the heat source and sink (see fig. 1), and it can be analyzed within the linear irreversible framework [42,43]. In the first stage, the heat flux $\dot{Q}_h$ enters the engine from the hot reservoir, power P is generated, and a heat flux $\dot{Q}_c$ goes into the finite sink whose instantaneous temperature T satisfies $T_c \leq T \leq T_h$.

Let, at some instant, $\mathrm{d}W$ be the infinitesimal work performed by the engine on the environment against a uniform external force F. Then, $\mathrm{d}W = -F\mathrm{d}x$, where x is the conjugate thermodynamic variable of F. The power output is $P = -F\dot{x} = \dot{Q}_h - \dot{Q}_c$. The instantaneous total entropy production rate in the reservoirs [15,35] is

$$\dot{S} = \frac{\dot{Q}_c}{T} - \frac{\dot{Q}_h}{T_h}, \tag{2}$$

$$= \frac{F\dot{x}}{T} + \dot{Q}_h \left(\frac{1}{T} - \frac{1}{T_h} \right). \tag{3}$$

Here, we can identify two thermodynamic force-flux pairs: $X_1 \equiv F/T$, $J_1 \equiv \dot{x}$, $X_2 \equiv 1/T - 1/T_h$, $J_2 \equiv \dot{Q}_h$ [15].

Then, we can write $\dot{S} = J_1 X_1 + J_2 X_2$, and $P = -T J_1 X_1$. If the thermodynamic forces are small, then the fluxes can be expressed in the following form [42,43]:

$$J_1 = L_{11} X_1 + L_{12} X_2, \tag{4}$$

$$J_2 = L_{21} X_1 + L_{22} X_2, \tag{5}$$

where $L_{ij}(i,j = 1,2)$ are the Onsager coefficients satisfying the reciprocity relation $L_{12} = L_{21}$, and $L_{12}L_{21} \leq L_{11}L_{22}$. Using eq. (4), the power output can be expressed in terms of J_1 as

$$P = \frac{L_{12}}{L_{11}} T X_2 J_1 - \frac{T}{L_{11}} J_1^2. \tag{6}$$

The input heat flux becomes

$$J_2 = \frac{L_{12}}{L_{11}} J_1 + L_{22}(1 - q^2) X_2, \tag{7}$$

where the coupling parameter, $q^2 \equiv L_{12}^2/(L_{11}L_{22})$, satisfies $0 \leq q^2 \leq 1$ [44]. Using eqs. (6) and (7), we can write $\dot{Q}_c \equiv J_3 = J_2 - P$ as

$$J_3 = \frac{L_{12}T}{L_{11}T_h} J_1 + L_{22}(1 - q^2) X_2 + \frac{T}{L_{11}} J_1^2. \tag{8}$$

Now, the rate of change of the sink temperature is given by $C_V \dot{T} = J_3$, where $\dot{T} > 0$. Solving for J_1 from eq. (8) and substituting in eq. (7), we get the input heat flux as a function of the form $J_2(T,\dot{T})$. Here, we discuss only the tight-coupling condition, $q^2 = 1$, which is analytically amenable. Finally, we obtain

$$J_2 = \frac{L_{22}}{2T_h} \left(\sqrt{1 + \frac{4T_h^2 C_V \dot{T}}{L_{22}T}} - 1 \right). \tag{9}$$

We assume that the finite-sized sink takes a time τ_h to reach thermal equilibrium with the hot reservoir. The work output in the first stage is given by

$$W = \int_0^{\tau_h} J_2 \mathrm{d}t - \int_0^{\tau_h} J_3 \mathrm{d}t = \int_0^{\tau_h} J_2 \mathrm{d}t - \Delta U, \tag{10}$$

where $\Delta U = \int_{T_c}^{T_h} C_V \dot{T} \mathrm{d}t$.

Optimization. – In order to maximize W, the input heat $Q_h \equiv \int_0^{\tau_h} J_2 \mathrm{d}t$ needs to be maximized. The corresponding Euler-Lagrange (EL) equation for the flux J_2 is given by

$$\frac{\mathrm{d}}{\mathrm{d}t} \left(\frac{\partial J_2}{\partial \dot{T}} \right) - \frac{\partial J_2}{\partial T} = 0. \tag{11}$$

Now, the Onsager coefficient L_{22} and heat capacity C_V may depend on the temperature. Even the above EL equation seems difficult to solve. To simplify, we assume $\frac{4T_h^2 C_V \dot{T}}{L_{22}T} \ll 1$ (see appendix A for the justification of this

approximation). Then, the input heat flux is approximated up to second order as

$$J_2 \approx C_V T_h \frac{\dot{T}}{T} - \frac{C_V^2 T_h^3}{L_{22}} \left(\frac{\dot{T}}{T} \right)^2. \tag{12}$$

The EL equation yields

$$\frac{2C_V^2}{L_{22}} \frac{\ddot{T}}{T^2} + \frac{\partial}{\partial T} \left(\frac{C_V^2}{L_{22}T^2} \right) \dot{T}^2 = 0. \tag{13}$$

Multiplying eq. (13) by $\dot{T}$ and simplifying, we can get

$$\frac{d}{dt} \left(\frac{C_V^2 \dot{T}^2}{L_{22}T^2} \right) = 0. \tag{14}$$

Integrating the above equation w.r.t. time, we get

$$\frac{C_V \dot{T}}{\sqrt{L_{22}}T} = A, \tag{15}$$

where $A > 0$ is a constant of integration. Then, integrating eq. (15) with respect to time, we get $A = B/\tau_h$, where $B = \int_{T_c}^{T_h} \frac{C_V}{\sqrt{L_{22}}T} dT > 0$. The input heat becomes

$$Q_h = T_h \int_{T_c}^{T_h} \frac{C_V dT}{T} - T_h^3 A^2 \int_0^{\tau_h} dt, \tag{16}$$

$$= T_h \Delta S - \frac{T_h^3 B^2}{\tau_h}, \tag{17}$$

where $\int_{T_c}^{T_h} \frac{C_V}{T} dT = \Delta S > 0$ is the entropy injected into the system in the first stage. Then, eq. (10) is evaluated to be

$$W = T_h \Delta S - \frac{T_h^3 B^2}{\tau_h} - \Delta U, \tag{18}$$

$$\equiv W_1 - \frac{T_h^3 B^2}{\tau_h}. \tag{19}$$

Clearly, as the time duration of the first stage diverges, the work output approaches its maximal value W_1. Upon rewriting eq. (17) as

$$\Delta S - \frac{Q_h}{T_h} = \frac{T_h^2 B^2}{\tau_h} > 0, \tag{20}$$

we note that the left-hand side of the above equation is the sum of the entropy changes in the sink and the hot reservoir, and so, it is equal to the total entropy generated due to the engine. In fact, the inverse proportionality of this quantity on the duration of the process is the basic assumption of the low-dissipation model [19].

After completing the first stage, the finite-sized system (now to be used as a heat source) is instantaneously connected with the cold reservoir via a linear irreversible heat engine. The heat extracted from the hot source successively decreases its temperature and we assume that, in a given time τ_c, the source reaches equilibrium with the cold reservoir (see fig. 1). The rate of change of the source temperature can be written as $-C_V \dot{T}' = J_2'$, where $\dot{T}' < 0$ denotes the rate of decrease of the source temperature. Thus, the total heat absorbed by the heat engine from the source (in the second stage) can be obtained as $Q_h' = \Delta U$. The optimized heat rejected to the cold reservoir (that maximizes the work extraction) can be calculated along similar lines [35]:

$$Q_c' = T_c \Delta S + \frac{T_c B'^2}{\tau_c}, \tag{21}$$

where $B' = \int_{T_c}^{T_h} \frac{C_V}{\sqrt{L_{22}'}} dT'$. Thus, the maximum work output in the second stage is given by [35]

$$W' = \Delta U - T_c \Delta S - \frac{T_c B'^2}{\tau_c}, \tag{22}$$

$$\equiv W_2 - \frac{T_c B'^2}{\tau_c}. \tag{23}$$

From eq. (21), we note that Q_c'/T_c is the entropy added reversibly to the cold reservoir, while ΔS is the change (decrease) in the entropy of the finite source. Thus, $Q_c'/T_c - \Delta S = B'^2/\tau_c$, is identified as the entropy generated in the second stage, which is also inversely proportional to the time τ_c spent on the process. Thus, we conclude that our model in which the individual stages are optimized for maximum work extraction with given times, yields the low-dissipation behavior [19]. This is our first main result.

The total extracted work, $W_{\text{tot}} = W + W'$, is given by

$$W_{\text{tot}} = \Delta T \Delta S - \frac{T_h^3 B^2}{\tau_h} - \frac{T_c B'^2}{\tau_c}. \tag{24}$$

Now, the cycle lasts for a time $\tau = \tau_h + \tau_c$. Therefore, the power generated per cycle is $P = W_{\text{tot}}/\tau$. Maximizing the power with respect to τ_h and τ_c (for fixed values of T_h, T_c, and ΔS [19]), we obtain the optimal allocation of times as

$$\tau_h^\star = \frac{2T_h^3 B^2}{\Delta T \Delta S} \left(1 + \Gamma \sqrt{\frac{T_c}{T_h}} \right), \tag{25}$$

$$\tau_c^\star = \frac{2T_c B'^2}{\Delta T \Delta S} \left(1 + \frac{1}{\Gamma} \sqrt{\frac{T_h}{T_c}} \right), \tag{26}$$

where $\Gamma = B'/(T_h B)$. The efficiency at maximum power is

$$\eta_{\text{MP}} = \eta_{\text{C}} \left(2 - \frac{\eta_{\text{C}}}{1 + \Gamma \sqrt{1 - \eta_{\text{C}}}} \right)^{-1}. \tag{27}$$

We note that Γ is determined by two kinds of control parameters: the thermostatic property (heat capacity) of the auxiliary system and thermal conductivities of the contacts with reservoirs (through L_{22} and L_{22}'). To analyze the dependence on these factors, we consider the following case.
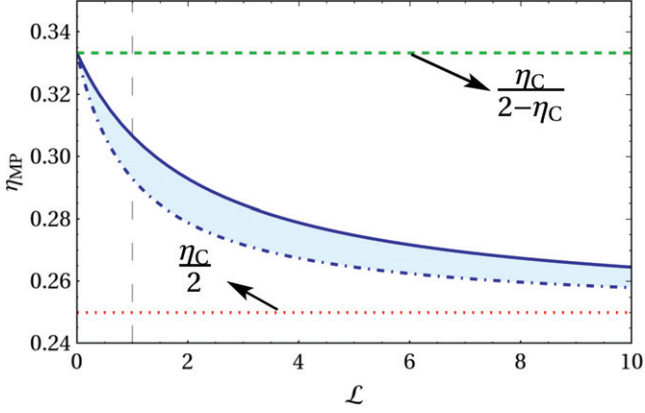
Fig. 2: The bounds of η_{MP} as given in eq. (28) (shaded region) plotted as a function of $\mathcal{L}$, for $\eta_{\mathrm{C}} = 0.5$. The upper (dashed) and the lower (dotted) horizontal lines are the bounds in eq. (29), towards which η_{MP} tends as $\mathcal{L} \to 0$ and $\mathcal{L} \to \infty$ respectively. The vertical large-dashed line represents the symmetric case $\mathcal{L} = 1$ ($L_{22} = L'_{22}$).

Special case. − In the near-equilibrium linear regime, we may take L_{22} and L'_{22} to be constant parameters (independent of temperature) [45]. Then, we denote $\mathcal{L} \equiv \sqrt{L_{22}/L'_{22}}$, and $T_m = \Delta U/\Delta S$, so that $\Gamma = \mathcal{L} T_m/T_h$. From the mathematical properties of the function $U(S)$ and the mean-value theorem [39], we know that T_m is bounded as: $T_c < T_m < T_h$. For a given $\mathcal{L}$, as $T_m \to T_c$ ($T_m \to T_h$), we obtain the upper (lower) bounds for η_{MP},

$$\frac{\eta_{\mathrm{C}}}{2 - \frac{\eta_{\mathrm{C}}}{1 + \mathcal{L}\sqrt{1 - \eta_{\mathrm{C}}}}} < \eta_{\mathrm{MP}} < \frac{\eta_{\mathrm{C}}}{2 - \frac{\eta_{\mathrm{C}}}{1 + \mathcal{L}(1 - \eta_{\mathrm{C}})\sqrt{1 - \eta_{\mathrm{C}}}}}. \quad (28)$$

On the other hand, the parameter $\mathcal{L}$ can take values in the range $0 < \mathcal{L} < \infty$. Further, η_{MP} decreases monotonically as $\mathcal{L}$ increases. Due to these conditions, the global bounds on EMP are as follows:

$$\frac{\eta_{\mathrm{C}}}{2} < \eta_{\mathrm{MP}} < \frac{\eta_{\mathrm{C}}}{2 - \eta_{\mathrm{C}}}, \quad (29)$$

where the lower (upper) bound is approached when $L_{22} \gg L'_{22}$ or $\mathcal{L} \to \infty$ ($L_{22} \ll L'_{22}$ or $\mathcal{L} \to 0$). The bounds from eqs. (28) and (29) are plotted in fig. 2.

In particular, we consider the symmetric situation where $L_{22}(T)$ and $L'_{22}(T')$ have the same functional form. Then, from the bounds on Γ (see appendix B), eq. (27) yields the following upper and lower bounds of the EMP:

$$1 - \sqrt{1 - \eta_{\mathrm{C}}} < \eta_{\mathrm{MP}}^{(\mathrm{sym})} < \frac{\eta_{\mathrm{C}}}{2 - \frac{\eta_{\mathrm{C}}}{1 + (1 - \eta_{\mathrm{C}})\sqrt{1 - \eta_{\mathrm{C}}}}}, \quad (30)$$

which is our second main result. The above bounds are depicted in fig. 3 (shaded region). We note that, in the symmetric case, we have a class of efficiencies which satisfy the criterion of universality up to the second order, i.e., $\eta_{\mathrm{MP}}^{(\mathrm{sym})} = \eta_C/2 + \eta_C^2/8 + O[\eta_C^3]$. Interestingly, the CA-efficiency emerges as the lower bound for EMP in the symmetric case.

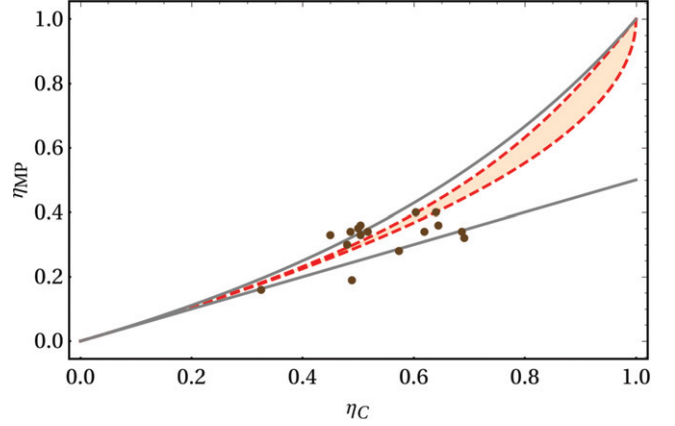Fig. 3: Bounds on EMP of the two-stage heat cycle plotted against Carnot value η_{C}. Upper and lower solid curves are as given in eq. (29). The dashed lines depict the bounds of $\eta_{\mathrm{MP}}^{(\mathrm{sym})}$ as in eq. (30), the lower being the CA-efficiency. The shaded region defines efficiencies under the symmetry condition $L_{22}(T) \equiv L'_{22}(T')$, which show universality up to the second order in η_{C}. The dots represent data on the observed efficiencies of a few thermal and nuclear plants as in ref. [46].

In order to study how η_{MP} depends upon the nature of the finite-sized heat source/sink, we assume a general form of the heat capacity, $C_V = \beta T^{\alpha}$, where β and α are constants depending upon the model system[1]. Then, we obtain

$$\eta_{\mathrm{MP}} = \frac{\eta_{\mathrm{C}}}{2 - \eta_{\mathrm{C}} \left[1 + \mathcal{L} \left(\frac{\alpha}{\alpha+1} \frac{1 - (1 - \eta_{\mathrm{C}})^{\alpha+1}}{1 - (1 - \eta_{\mathrm{C}})^{\alpha}}\right) \sqrt{1 - \eta_{\mathrm{C}}}\right]^{-1}}. \quad (31)$$

Expanding the above η_{MP} in terms of η_{C}, we get

$$\eta_{\mathrm{MP}} = \frac{\eta_{\mathrm{C}}}{2} + \frac{\eta_{\mathrm{C}}^2}{4(1 + \mathcal{L})} + \frac{1 + 2\mathcal{L}}{8(1 + \mathcal{L})^2}\eta_{\mathrm{C}}^3$$
$$+ \frac{6 + (23 - 2\alpha)(1 + \mathcal{L})\mathcal{L}}{96(1 + \mathcal{L})^3}\eta_{\mathrm{C}}^4 + \mathcal{O}[\eta_{\mathrm{C}}^5], \quad (32)$$

which shows that the efficiency at maximum power depends only weakly on the nature of the auxiliary system.

Conclusions. − We have proposed a two-stage heat cycle with a finite time period, where an auxiliary system plays the role of a finite sink in one stage and a finite heat source in the other stage. In each stage, a linear irreversible engine, coupled to the finite system and one of the heat reservoirs, is optimized for maximum work output in a given time. The usual formulations of finite-time Carnot engines involve four stages where, for simplification, the time spent on adiabatic stages is often assumed to be negligible [9,16,19] (see also footnote [2]). In this regard, note that the proposed model does not involve any

---

[1]For instance, for an ideal monatomic gas, $\beta = 3N\kappa_B/2$, and $\alpha = 0$. For solids at low temperatures, $\beta = 12\pi^4 N\kappa_B/(5\Theta_D)$ and $\alpha = 3$, where N, κ_B and Θ_D are the number of particles, Boltzmann constant and the Debye temperature, respectively.

[2]It may be noted that some studies have inclued adiabatic times in the four-step low-dissipation models [47,48], and the obtained

adiabatic stages. Also, the model does not depend on special conditions such as endoreversibility [2,5].

It is observed that under the tight-coupling condition, the present model is formally analogous to the low-dissipation model [19]. In fact, the dissipation constants that are introduced phenomenologically in the latter model are determined within the theory in terms of heat transfer coefficients and heat capacity of the auxiliary system. It is to be noted that LD behaviour has been derived both within classical or quantum domains with mesoscopic or quantum systems [16,49,50] and also observed experimentally [51,52]. However, a basic derivation of this behavior for classical, macroscopic engines is not known. The present model provides a foundation for the low-dissipation assumption for *macroscopic* thermal machines [19], based on notions from linear irreversible thermodynamics.

Now, it is well known that for a linear irreversible engine, coupled simultaneously with the infinite-sized hot and cold reservoirs, the efficiency at maximum power is bounded from above by one-half of the Carnot value [15]. The main outcome of our study is that if the engine is designed to operate with an additional finite-sized reservoir which alternately acts as a finite heat source and sink, then the efficiency at maximum power can surpass the upper bound mentioned above (see eq. (32)).

Further, the efficiency at maximum power is found to be consistent with the universal properties of efficiency observed in other models. In contrast to the low-dissipation model where CA-efficiency is obtained under the symmetric condition [19], here we get a class of efficiencies with CA-efficiency being the lower bound. Curiously, we note that though the observed efficiencies of quite a few well-known plants fall within the bounds (eq. (29)), the available data seem to be excluded from the region of symmetry (shaded area in fig. 3). This suggests that the symmetric situation may not be a preferred design, although it would be a simpler choice. This observation might also indicate that power optimization is not a common objective for the various power plants. On the other hand, real heat engines may work at a trade-off between power and efficiency [10,19,53–61]. Particularly, under the symmetric condition, the performance of such models at the maximum trade-off criterion explains the observed power plants quite well [48,54,57]. Finally, among other generalizations, it will be interesting to extend the model beyond the linear regime [21,62], as well as for refrigerators [63,64].

$$* * *$$

Appendix A: input heat flux approximation. – The input heat flux in the first stage is given by (eq. (9))

$$J_2 = \frac{L_{22}}{2T_h}\left[\sqrt{1 + \frac{4T_h^2 C_V \dot{T}}{L_{22}T}} - 1\right]. \qquad (A.1)$$

Here, the Onsager coefficient $L_{22} \geq 0$ and the rate of change of temperature of the finite-size sink, $\dot{T} \geq 0$. When the quantity $\frac{4T_h^2 C_V \dot{T}}{L_{22}T} \ll 1$, the input heat flux can be approximated as

$$J_2 \approx C_V T_h \frac{\dot{T}}{T} - \frac{C_V^2 T_h^3}{L_{22}}\left(\frac{\dot{T}}{T}\right)^2, \qquad (A.2)$$

which gives the following optimal rate of change for the temperature (eq. (15)):

$$\frac{C_V \dot{T}}{\sqrt{L_{22}}T} = A = \frac{B}{\tau_h}. \qquad (A.3)$$

Therefore, the quantity

$$\frac{4T_h^2 C_V \dot{T}}{L_{22}T} = \frac{4T_h^2 B}{\sqrt{L_{22}}\tau_h}. \qquad (A.4)$$

For a constant L_{22}, we get $B = \Delta S/\sqrt{L_{22}}$, where $\Delta S \equiv \int_{T_c}^{T_h}(C_V/T)\mathrm{d}T$. Rewriting the above equation

$$\frac{4T_h^2 C_V \dot{T}}{L_{22}T} = \frac{4T_h^2 \Delta S}{L_{22}\tau_h}. \qquad (A.5)$$

Thus, our approximation implies the following condition:

$$\frac{4T_h^2 \Delta S}{L_{22}\tau_h} \ll 1, \qquad (A.6)$$

which requires a sufficiently long duration for the first stage, given the values of other parameters.

Further, the consistency of our approximation can be checked with the optimal power solution, for which we obtained the optimal time τ_h as

$$\tau_h^\star = \frac{2T_h^3 B^2}{\Delta T \Delta S}(1 + \Gamma\sqrt{\theta}) = \frac{2T_h^3 \Delta S}{L_{22}\Delta T}(1 + \Gamma\sqrt{\theta}), \qquad (A.7)$$

where $\Gamma \equiv B'/(T_h B)$ and $\theta \equiv T_c/T_h$. Substituting the above $\tau_h^\star$ in eq. (A.5), we get

$$\frac{4T_h^2 C_V \dot{T}}{L_{22}T} = \frac{2\Delta T}{T_h}\frac{1}{(1 + \Gamma\sqrt{\theta})}. \qquad (A.8)$$

Since $\Delta T \ll T_h$ in the linear irreversible regime, it follows that

$$\frac{4T_h^2 C_V \dot{T}}{L_{22}T} \ll 1. \qquad (A.9)$$

results provide good indicators of the performance of the real refrigerators [48].

Appendix B: bounds on parameter Γ for the symmetric case. – Let us consider the inequality

$$m \int_a^b g(x)\mathrm{d}x \le \int_a^b f(x)g(x)\mathrm{d}x \le M \int_a^b g(x)\mathrm{d}x, \quad \text{(B.1)}$$

with $m \le f(x) \le M$. Assuming the functions $f(x)$ and $g(x)$ to be integrable between the limits a and b, we take the symmetric situation where $L_{22}(T) \equiv L'_{22}(T')$ and $T_c \le T \le T_h$. Therefore, we can write

$$\frac{1}{T_h} \int_{T_c}^{T_h} \frac{C_V \mathrm{d}T}{\sqrt{L_{22}}} \le \int_{T_c}^{T_h} \frac{C_V \mathrm{d}T}{\sqrt{L_{22}T}} \le \frac{1}{T_c} \int_{T_c}^{T_h} \frac{C_V \mathrm{d}T}{\sqrt{L_{22}}}. \quad \text{(B.2)}$$

Using the definitions of B and B', we get

$$\frac{B'}{T_h} \le B \le \frac{B'}{T_c}. \quad \text{(B.3)}$$

Rewriting the above equation, we get the bounds as

$$\frac{T_c}{T_h} \le \Gamma \le 1. \quad \text{(B.4)}$$

REFERENCES

[1] CARNOT S., *Réflexions sur la Puissance Motrice du Feu, et sur les Machines Propres à Développer cette Puissance*, 1824.
[2] CURZON F. L. and AHLBORN B., *Am. J. Phys.*, **43** (1975) 22.
[3] ANDRESEN B., SALAMON P. and BERRY R. S., *J. Chem. Phys.*, **66** (1977) 1571.
[4] ANDRESEN B., BERRY R. S., NITZAN A. and SALAMON P., *Phys. Rev. A*, **15** (1977) 2086.
[5] RUBIN M. H., *Phys. Rev. A*, **19** (1979) 1272.
[6] SALAMON P., NITZAN A., ANDRESEN B. and BERRY R. S., *Phys. Rev. A*, **21** (1980) 2115.
[7] ANDRESEN B., SALAMON P. and BERRY R. S., *Phys. Today*, **64** (1984) 62.
[8] DE VOS A., *Am. J. Phys.*, **53** (1985) 570.
[9] CHEN L. and YAN Z., *J. Chem. Phys.*, **90** (1989) 3740.
[10] ANGULO-BROWN F., *J. Appl. Phys.*, **69** (1991) 7465.
[11] CHEN J., *J. Phys. D: Appl. Phys.*, **27** (1994) 1144.
[12] BEJAN A., *J. Appl. Phys.*, **79** (1996) 1191.
[13] CHEN L., SUN F. and WU C., *J. Phys. D: Appl. Phys.*, **32** (1999) 99.
[14] SALAMON P. and NITZAN A., *J. Chem. Phys.*, **74** (1981) 3546.
[15] VAN DEN BROECK C., *Phys. Rev. Lett.*, **95** (2005) 190602.
[16] SCHMIEDL T. and SEIFERT U., *EPL*, **81** (2008) 20003.
[17] TU Z. C., *J. Phys. A*, **41** (2008) 312003.
[18] ESPOSITO M., LINDENBERG K. and VAN DEN BROECK C., *Phys. Rev. Lett.*, **102** (2009) 130602.
[19] ESPOSITO M., KAWAI R., LINDENBERG K. and VAN DEN BROECK C., *Phys. Rev. Lett.*, **105** (2010) 150603.
[20] BENENTI G., SAITO K. and CASATI G., *Phys. Rev. Lett.*, **106** (2011) 230602.
[21] IZUMIDA Y. and OKUDA K., *EPL*, **97** (2012) 10004.
[22] BRANDNER K., SAITO K. and SEIFERT U., *Phys. Rev. Lett.*, **110** (2013) 070603.
[23] HOLUBEC V., *J. Stat. Mech.*, **2014** (2014) 05022.
[24] TU Z. C., *Phys. Rev. E*, **89** (2014) 052148.
[25] VAUDREY A., LANZETTA F. and FEIDT M., *J. Noneq. Therm.*, **39** (2014) 199.
[26] JIANG J.-H., *Phys. Rev. E*, **90** (2014) 042126.
[27] BAUER M., BRANDNER K. and SEIFERT U., *Phys. Rev. E*, **93** (2016) 042112.
[28] BRANDNER K., SAITO K. and SEIFERT U., *Phys. Rev. X*, **5** (2015) 031019.
[29] PROESMANS K., CLEUREN B. and VAN DEN BROECK C., *Phys. Rev. Lett.*, **116** (2016) 220601.
[30] PROESMANS K., DREHER Y., GAVRILOV M., BECHHOEFER J. and VAN DEN BROECK C., *Phys. Rev. X*, **6** (2016) 041010.
[31] RYABOV A. and HOLUBEC V., *Phys. Rev. E*, **93** (2016) 050101(R).
[32] JOHAL R. S., *Phys. Rev. E*, **96** (2017) 012151.
[33] DECHANT A., KIESEL N. and LUTZ E., *EPL*, **119** (2017) 50003.
[34] JOHAL R. S., *EPL*, **121** (2018) 50009.
[35] IZUMIDA Y. and OKUDA K., *Phys. Rev. Lett.*, **112** (2014) 180603.
[36] WANG Y., *Phys. Rev. E*, **90** (2014) 062140.
[37] WANG Y., *Phys. Rev. E*, **93** (2016) 012120.
[38] JOHAL R. S. and RAI R., *EPL*, **113** (2016) 10006.
[39] JOHAL R. S., *Phys. Rev. E*, **94** (2016) 012123.
[40] MA Y.-H., *Effect of finite-size heat source's heat capacity on the efficiency of heat engine*, arXiv preprint, arXiv:1910.13690 (2019).
[41] MORAN M. J., SHAPIRO H. N., BOETTNER D. D. and BAILEY M. B., *Fundamentals of Engineering Thermodynamics*, 7th edition (John Wiley & Sons, Inc., USA) 2011, p. 362.
[42] ONSAGER L., *Phys. Rev.*, **38** (1931) 2265.
[43] CALLEN H. B., *Thermodynamics and an Introduction to Thermostatistics*, 2nd edition (John Wiley & Sons, New York) 1985, p. 312.
[44] KEDEM O. and CAPLAN S. R., *Trans. Faraday Soc.*, **61** (1965) 1897.
[45] KONDEPUDI D. and PRIGOGINE I., *Modern Thermodynamics: From Heat Engines to Dissipative Structures*, 2nd edition (John Wiley & Sons Ltd., West Sussex) 2015, p. 364.
[46] JOHAL R. S., *Eur. Phys. J. ST*, **226** (2017) 489.
[47] WANG J. and HE J., *Phys. Rev. E*, **86** (2012) 051112.
[48] HU Y., WU F., MA Y., HE J., WANG J., CALVO HERNÁNDEZ A. and ROCO J. M. M., *Phys. Rev. E*, **88** (2013) 062115.
[49] ESPOSITO M., KAWAI R., LINDENBERG K. and VAN DEN BROECK C., *Phys. Rev. E*, **81** (2010) 041106.
[50] CAVINA V., MARI A. and GIOVANNETTI V., *Phys. Rev. Lett.*, **119** (2017) 050601.
[51] MARTÍNEZ I. A., ROLDÁN É., DINIS L., PETROV D., PARRONDO J. M. R. and RICA R. A., *Nat. Phys.*, **12** (2016) 67.
[52] MA Y.-H., ZHAI R.-X., SUN C.-P. and DONG H., *Experimental validation of the $1/\tau$-scaling entropy generation in finite-time thermodynamics with dry air*, arXiv preprint, arXiv:1910.13434 (2019).
[53] ANGULO-BROWN F., SANTILLÁN M. and CALLEJA-QUEVEDO E., *Nuovo Cimento D*, **17** (1995) 87.

[54] DE TOMÁS C., CALVO HERNÁNDEZ A. and ROCO
J. M. M., *Phys. Rev. E*, **85** (2012) 010104.

[55] CALVO HERNÁNDEZ A., MEDINA A., ROCO J. M. M.,
WHITE J. A. and VELASCO S., *Phys. Rev. E*, **63** (2001)
037102.

[56] SÁNCHEZ-SALAS N., LÓPEZ-PALACIOS L., VELASCO S.
and CALVO HERNÁNDEZ A., *Phys. Rev. E*, **82** (2010)
051101.

[57] LONG R., LIU Z. and LIU W., *Phys. Rev. E*, **89** (2014)
062119.

[58] GONZALEZ-AYALA J., CALVO HERNÁNDEZ A. and ROCO
J. M. M., *Phys. Rev. E*, **95** (2017) 022131.

[59] IYYAPPAN I. and PONMURUGAN M., *J. Stat. Mech.*, **2017**
(2017) 093207.

[60] SINGH V. and JOHAL R. S., *Entropy*, **19** (2017) 576.

[61] IYYAPPAN I. and PONMURUGAN M., *J. Stat. Mech.*, **2018**
(2018) 033202.

[62] IZUMIDA Y., OKUDA K., ROCO J. M. M. and CALVO
HERNÁNDEZ A., *Phys. Rev. E*, **91** (2015) 052140.

[63] JIMÉNEZ DE CISNEROS B., ARIAS-HERNÁNDEZ L. A.
and CALVO HERNÁNDEZ A., *Phys. Rev. E*, **73** (2006)
057103.

[64] IZUMIDA Y., OKUDA K., CALVO HERNÁNDEZ A. and
ROCO J. M. M., *EPL*, **101** (2013) 10005.